

## RESEARCH ARTICLE

# Enhancement of acyl-CoA precursor supply for increased avermectin B1a production by engineering meilingmycin polyketide synthase and key primary metabolic pathway genes

Mengyao Yang<sup>1</sup> | Yi Hao<sup>1</sup> | Gang Liu<sup>2</sup>  | Ying Wen<sup>1</sup> 

<sup>1</sup>State Key Laboratory of Animal Biotech Breeding and College of Biological Sciences, China Agricultural University, Beijing, China

<sup>2</sup>State Key Laboratory of Mycology, Institute of Microbiology, Chinese Academy of Sciences, Beijing, China

## Correspondence

Ying Wen, State Key Laboratory of Animal Biotech Breeding and College of Biological Sciences, China Agricultural University, Beijing 100193, China.  
Email: [wen@cau.edu.cn](mailto:wen@cau.edu.cn)

## Funding information

National Key Research and Development Program of China, Grant/Award Number: 2021YFC2100600 and 2023YFC3402400

## Abstract

Avermectins (AVEs), a family of macrocyclic polyketides produced by *Streptomyces avermitilis*, have eight components, among which B1a is noted for its strong insecticidal activity. Biosynthesis of AVE “a” components requires 2-methylbutyryl-CoA (MBCoA) as starter unit, and malonyl-CoA (MalCoA) and methylmalonyl-CoA (MMCoA) as extender units. We describe here a novel strategy for increasing B1a production by enhancing acyl-CoA precursor supply. First, we engineered meilingmycin (MEI) polyketide synthase (PKS) for increasing MBCoA precursor supply. The loading module (using acetyl-CoA as substrate), extension module 7 (using MMCoA as substrate) and TE domain of MEI PKS were assembled to produce 2-methylbutyrate, providing the starter unit for B1a production. Heterologous expression of the newly designed PKS (termed Mei-PKS) in *S. avermitilis* wild-type (WT) strain increased MBCoA level, leading to B1a titer 262.2 µg/mL – 4.36-fold higher than WT value (48.9 µg/mL). Next, we separately inhibited three key nodes in essential pathways using CRISPRi to increase MalCoA and MMCoA levels in WT. The resulting strains all showed increased B1a titer. Combined inhibition of these key nodes in Mei-PKS expression strain increased B1a titer to 341.9 µg/mL. Overexpression of fatty acid β-oxidation pathway genes in the strain further increased B1a titer to 452.8 µg/mL – 8.25-fold higher than WT value. Finally, we applied our precursor supply strategies to high-yield industrial strain A229. The strategies, in combination, led to B1a titer 8836.4 µg/mL – 37.8% higher than parental A229 value. These findings provide an effective combination strategy for increasing AVE B1a production in WT and industrial *S. avermitilis* strains, and our precursor supply strategies can be readily adapted for overproduction of other polyketides.

## INTRODUCTION

Polyketides are useful secondary metabolites that display great structural diversity and are widely applied in medicine, industry, and agriculture. The majority are produced by actinomycetes, particularly *Streptomyces*

species. Examples include anticancer drugs (doxorubicin, bleomycin), antibiotics (erythromycin, tetracycline), antifungals (amphotericin B), antiparasitics (avermectins, meilingmycins), and immunosuppressants (rapamycin, FK506) (Li et al., 2021). Polyketides are synthesized by polyketide synthases (PKSs) through repeated Claisen

This is an open access article under the terms of the [Creative Commons Attribution-NonCommercial](https://creativecommons.org/licenses/by-nc/4.0/) License, which permits use, distribution and reproduction in any medium, provided the original work is properly cited and is not used for commercial purposes.

© 2024 The Authors. *Microbial Biotechnology* published by John Wiley & Sons Ltd.

condensation reaction of acyl-CoA extender units onto the starter unit. Many polyketides are synthesized by multimodular enzyme complexes called type I modular PKSs. Such PKS consists of a series of modules, each of which controls a single round of chain elongation steps. A minimal module consists of a ketosynthase (KS) domain that catalyses decarboxylative carbon-carbon bond formation between an incoming acyl-CoA unit and a polyketide intermediate, an acyltransferase (AT) domain that determines the specific acyl-CoA incorporated into the polyketide chain, and an acyl carrier protein (ACP) domain that functions as a carrier for incoming acyl-CoA units and extended chains. Presence of reductive domains within different modules varies. If present, the ketoreductase (KR) domain converts  $\beta$ -ketone to an alcohol, the dehydratase (DH) domain eliminates alcohol to form an olefin, and the enoylreductase (ER) domain reduces olefin to a methylene. This incorporation/condensation/reduction cycle is repeated by downstream modules, and leads eventually to release of a large, complex polyketide chain by a thioesterase (TE) domain located at the PKS terminus (Barajas et al., 2017). Engineering of type I PKSs, based on this collinear biosynthetic logic, has the potential to generate a huge variety of rationally designed compounds. Hagen et al. (2014, 2016), for example, introduced heterologous reductive domains into the first extension module of borrelidin PKS and attached a TE domain to construct a hybrid PKS capable of producing free adipic acid in vitro. Yuzawa et al. (2018) produced industrially relevant short-chain ketones in *S. albus* using a hybrid PKS. Kudo et al. (2020) applied Cas9 reaction and Gibson assembly to edit rapamycin PKS gene in vitro and produced desired rapamycin derivatives in industrial species *S. avermitilis* through heterologous expression of the edited PKS gene.

Avermectins (AVEs) are a family of 16-membered macrocyclic polyketides, produced by *S. avermitilis*, that were characterized in the 1970s and found to have strong anthelmintic and insecticidal properties. AVEs are comprised of four major components (A1a, A2a, B1a, B2a) and four minor components (A1b, A2b, B1b, B2b). Of these, B1a displays the highest insecticidal activity and lowest toxicity in humans and other mammals (Burg et al., 1979; Egerton et al., 1979). AVEs and their derivatives (ivermectin, doramectin, eprinomectin emamectin, emamectin benzoate, selamectin) are used worldwide as pesticides (El-Saber Batiha et al., 2020). A popular AVE commercial product called abamectin is a mixture of B1a (>80%) and B1b (<20%). AVEs are synthesized by type I PKS, which utilizes 2-methylbutyryl-CoA (MBCoA) (for “a” components) or isobutyryl-CoA (IsoBuCoA) (for “b” components) as starter unit, and seven malonyl-CoAs (MalCoAs) and five methylmalonyl-CoAs (MMCoAs) as extender units, to form a macrolide skeleton (Yoon et al., 2004). Modifications of this macrolide give rise to AVE aglycones, which undergo further glycosylation to produce

final AVEs (Ikeda et al., 1999, 2001). Increase of acyl-CoA precursor supply is a promising strategy for enhancement of polyketide production (Li et al., 2021). Increase of MBCoA supply should theoretically lead to increased production of AVE “a” components and consequently of B1a. However, an effective method for increasing intracellular MBCoA level has not yet been developed.

Meilingmycins (MEIs), produced by *S. nanchangensis* NS3226, are another family of 16-membered macrolide antibiotics with similar polyketide skeleton and antiparasitic properties to those of AVEs (Sun et al., 2002). Biosynthesis of MEI A, B, D, and E is initiated with starter unit acetyl-CoA (AcCoA) by the loading module, followed by condensation of seven MalCoA and five MMCoA extender units (He et al., 2010). Deng et al. (2019) replaced the DH-KR domains of AVE PKS module 2 with MEI PKS module 2 reductive domains DH-ER-KR to produce ivermectin B1a. Based on the pioneering studies by Hagen et al. (2014, 2016) and Yuzawa et al. (2018), we attempted to construct a hybrid PKS capable of producing increased levels of MBCoA precursor for AVE B1a biosynthesis. Analysis of MEI biosynthesis processes suggests that if MEI PKS loading module (using AcCoA as substrate) is assembled with extension module 7 (using MMCoA as substrate) and TE domain, the resulting engineered PKS would catalyse production from substrates of 2-methylbutyrate, which would then be converted to MBCoA in cells, providing the starter unit for B1a production.

Polyketide acyl-CoA precursors are essential building blocks in cell growth, as well as common components in primary metabolic pathways such as tricarboxylic acid (TCA) cycle and fatty acid (FA) synthesis (Rokem et al., 2007). *Streptomyces* species typically switch metabolism to polyketide synthesis during stationary growth phases when external nutrients become limited (Wang et al., 2020). Because secondary metabolites are not required for cell growth but for host survival in adverse environments, the yields of polyketides are generally low and tightly regulated (Cao et al., 2020). Such low yield does not meet the requirement for large-scale industrial production. Strategies for yield improvement require coordination of cell growth with polyketide production (Li et al., 2021). Jones et al. (2011) demonstrated that knockout of *phaAB* genes (encoding forkhead-associated proteins) resulted in reduced TCA cycle activity and redirected carbon flux towards actinorhodin production. Wang et al. (2020) observed that degradation of intracellular triacylglycerol (TAG) pool during stationary growth phase provided acyl-CoA precursors necessary for polyketide production. Based on this finding, they developed a “dynamic degradation of TAG” (ddTAG) strategy using a cumate inducible system to mobilize TAG pool and redirect carbon flux towards polyketide production without reducing cell growth. AVE B1a production in industrial-scale fermentation

was significantly increased using this strategy. In a study by Tian et al. (2020), various essential genes involved in TCA cycle, FA synthesis, and aromatic amino acid synthesis pathways were downregulated in a cell density-dependent manner to redirect metabolic flux towards enhanced rapamycin production. These findings indicate the importance of redistributing precursors for increasing polyketide production.

Here, we describe enhancement of MBCoA precursor supply for AVE B1a production in *S. avermitilis* by heterologous expression of assembled loading module-extension module 7-TE domain of MEI PKS (a newly designed PKS, termed Mei-PKS). We increased MalCoA and MMCoA supplies through inhibition of three key nodes in FA synthesis and TCA cycle pathways using CRISPRi; *dcas9* was controlled by *S. avermitilis* native temporal promoter *pkn5p* (active mainly in middle and late fermentation stages). MalCoA, MMCoA, and MBCoA supplies were also increased through overexpression of FA  $\beta$ -oxidation pathway genes *fadD* and *fadAB* using *pkn5p* in the Mei-PKS expression strain. These precursor supply strategies, in combination, greatly enhanced B1a production in wild-type (WT) and industrial strains.

## EXPERIMENTAL PROCEDURES

### Plasmids, primers, bacterial strains, and culture conditions

Bacterial strains and plasmids used in this study are listed in Table S1, and primers are listed in Table S2. *Escherichia coli* JM109 was used as host strain for routine cloning, and *E. coli* ET12567 was used to propagate non-methylated DNA for transformation into *S. avermitilis* (Macneil & Klapko, 1987). Culture conditions for *E. coli* and *S. avermitilis* were described previously (Liu et al., 2015). For *S. nanchangensis* NS3226, YMS solid medium (Ikeda et al., 1988) was used for spore preparation, and YEME liquid medium (Kieser et al., 2000) was used to culture mycelia for DNA extraction. Insoluble fermentation medium FM-I (Jiang et al., 2011) was used for routine AVE production. Because dry cell weight is used as a measure of biomass and FM-I contains insoluble yeast meal, soluble fermentation medium FM-II (Jiang et al., 2011) was used to culture mycelia for growth analysis. AVE production was lower in FM-II than in FM-I.

### Construction of recombinant plasmids and *S. avermitilis* mutant strains

For heterologous expression of the newly designed Mei-PKS in *S. avermitilis*, DNA fragments *mei-LM* (1647 bp for the loading module), *mei-M7* (6426 bp for the seventh

extension module), and *mei-TE* (894 bp for the TE domain) were PCR amplified from genomic DNA of *S. nanchangensis* NS3226 using primer pairs YMY1A/YMY1B, YMY2A/YMY2B, and YMY3A/YMY3B, respectively. Promoter *aveBIIIp* was amplified from WT genomic DNA of *S. avermitilis* using primer pair YMY4A/YMY4B. Promoter *kasOp\** was amplified from pKC-*kasOp\**-*aveC8m* (Hao et al., 2022) with primer pair YMY5A/YMY5B. Promoter fragments *aveBIIIp* and *kasOp\** were assembled separately with *mei-LM* fragment by overlap extension PCR using primer pairs YMY4A/YMY1B and YMY5A/YMY1B. *aveBIIIp-me-LM* (or *kasOp\*-me-LM*), *mei-M7*, and *mei-TE* fragments were ligated into *NdeI*-digested integrative plasmid pIJ10500 (Pullan et al., 2011) using seamless assembly cloning kit (Clone Smarter; USA) to generate plasmids *paveBIIIp-me-pks* and *pkasOp\*-me-pks*, which were transformed separately into WT *S. avermitilis* to generate strains *aveBIIIp-me-pks* and *kasOp\*-me-pks*. *pkasOp\*-me-pks* was transformed into industrial strain A229 to generate *kasOp\*-me-pks/A229*.

For construction of CRISPRi plasmids, pSET-*pkn5p-dcas9* was constructed, based on pSET-*dcas9* (Zhao et al., 2018), by replacing *ermEp\** with *pkn5p* for dCas9 expression. In brief, promoter *pkn5p* was amplified from *S. avermitilis* WT DNA using primer pair YMY6A/YMY6B, and the resulting PCR product was digested with *XbaI/NdeI* and inserted into pSET-*dcas9* to generate pSET-*pkn5p-dcas9*. A 20-nt specific guide sequence ( $N_{20}$ ) of sgRNAs targeting non-template (NT) strand of genes of interest was designed using online software program CRISPy-web (<http://crispy.secondarymetabolites.org>) (Blin et al., 2016).  $N_{20}$  target sequences were synthesized by PCR annealing using forward primer (sgRNA-F) 5'-TAGTN<sub>20</sub>G-3' and reverse primer (sgRNA-R) 5'-AAAACN<sub>20</sub>-3', and ligated into *BsaI*-digested pSET-*pkn5p-dcas9* to construct CRISPRi plasmids *pfabH1<sup>i</sup>*, *pfabH2<sup>i</sup>*, *pfabH3<sup>i</sup>*, *pfabH4<sup>i</sup>*, *pfabD<sup>i</sup>*, *psucC1D1<sup>i</sup>*, *psucC2D2<sup>i</sup>*, *pfabH2<sup>i</sup>sucC2D2<sup>i</sup>*, *pfabD<sup>i</sup>sucC2D2<sup>i</sup>*, and *pfabH2<sup>i</sup>fabD<sup>i</sup>sucC2D2<sup>i</sup>*. *pfabH1<sup>i</sup>*, *pfabH2<sup>i</sup>*, *pfabH3<sup>i</sup>*, *pfabH4<sup>i</sup>*, *pfabD<sup>i</sup>*, *psucC1D1<sup>i</sup>*, and *psucC2D2<sup>i</sup>* were separately transformed into WT strain to generate corresponding strains *fabH1<sup>i</sup>*, *fabH2<sup>i</sup>*, *fabH3<sup>i</sup>*, *fabH4<sup>i</sup>*, *fabD<sup>i</sup>*, *sucC1D1<sup>i</sup>*, and *sucC2D2<sup>i</sup>*. *pfabH2<sup>i</sup>*, *pfabD<sup>i</sup>*, *psucC2D2<sup>i</sup>*, *pfabH2<sup>i</sup>sucC2D2<sup>i</sup>*, *pfabD<sup>i</sup>sucC2D2<sup>i</sup>*, and *pfabH2<sup>i</sup>fabD<sup>i</sup>sucC2D2<sup>i</sup>* were separately transformed into *kasOp\*-me-pks* to generate strains *fabH2<sup>i</sup>-pks*, *fabD<sup>i</sup>-pks*, *sucC2D2<sup>i</sup>-pks*, *fabH2<sup>i</sup>sucC2D2<sup>i</sup>-pks*, *fabD<sup>i</sup>sucC2D2<sup>i</sup>-pks*, and *fabH2<sup>i</sup>fabD<sup>i</sup>sucC2D2<sup>i</sup>-pks*. *pfabH2<sup>i</sup>fabD<sup>i</sup>sucC2D2<sup>i</sup>* was transformed into *kasOp\*-me-pks/A229* to generate strain *fabH2<sup>i</sup>fabD<sup>i</sup>sucC2D2<sup>i</sup>-pks/A229*.

For overexpression of *fadD* and *fadAB*, multicopy plasmid pOfadD-*fadAB* carrying *pkn5p*-driven *fadD* and *fadAB* (Hao et al., 2022) was transformed into *kasOp\*-me-pks* to generate strain OfadD-*fadAB-pks*. *pkn5p-fadD-fadAB* fragment was amplified using primer pair YMY7A/YMY7B from plasmid pOfadD-*fadAB*, and

ligated into *Xba*I-digested pfabH2<sup>i</sup>fabD<sup>i</sup>sucC2D2<sup>i</sup> to generate pOfad-fabH2<sup>i</sup>fabD<sup>i</sup>sucC2D2<sup>i</sup>, which was transformed separately into kasOp<sup>\*</sup>-mei-pks and kasOp<sup>\*</sup>-mei-pks/A229 to generate strains Ofad-fab<sup>i</sup>suc<sup>i</sup>-pks and Ofad-fab<sup>i</sup>suc<sup>i</sup>-pks/A229.

## RNA isolation and RT-qPCR analysis

Total RNAs of *S. avermitilis* were prepared from mycelia cultured in FM-I for various times, using TRIzol reagent (Tiangen; China). Contaminated genomic DNA from crude RNA samples was removed using DNase I (TaKaRa; China). Transcription levels of genes tested by RT-qPCR analysis were determined as described previously using sequence-specific primers listed in Table S2 (Luo et al., 2014). Relative expression level of each gene was calculated by comparative Ct method, and data were normalized relative to expression of internal control gene *hrdB* (*sav\_2444*). Experiments were performed in triplicate.

## Quantification of AVE B1a production

B1a production in fermentation broth of the various strains was quantified by HPLC as described previously (Luo et al., 2014).

## Extraction and detection of intracellular acyl-CoAs

*Streptomyces avermitilis* mycelia cultured in FM-I for various durations were ground in liquid nitrogen to fine powder. The powder was extracted with 10% trichloroacetic acid at 4°C, and the suspension was centrifuged (11,000 × *g*, 15 min, 4°C). Acyl-CoAs in the supernatant were detected by HPLC with C18 reverse-phase column (5 μm, 4.6 × 150 mm) and multiple-gradient elution procedure. MalCoA, MMCoA, and IsoBuCoA were detected by HPLC as described previously (Lyu et al., 2020). For detection of MBCoA, HPLC buffer A consisted of 200 mM sodium phosphate (pH 5.0), and buffer B consisted of 250 mM sodium phosphate (pH 5.0) and 20% acetonitrile. The column was equilibrated with 97% buffer A/3% buffer B at flow rate 1 mL/min. Samples were injected, and a linear gradient to 18% buffer B was generated over 5 min, followed by linear gradients to 28% over 2.5 min, to 40% over 5 min, to 42% over 5.5 min, and to 3% over 7 min. Detection wavelengths were 260 nm for MalCoA, MMCoA, and IsoBuCoA, and 254 nm for MBCoA. Authentic samples of MalCoA, MMCoA, IsoBuCoA (Sigma-Aldrich, USA), and MBCoA (synthesized by Shanghai Kai Sen Biotechnology Co.) were used as standards.

## RESULTS

### Rational engineering of MEI PKS for increasing MBCoA supply and AVE B1a production

The loading and seventh extension modules of MEI PKS (respectively termed Mei-LM and Mei-M7 hereafter) use AcCoA and MMCoA as starter and extender units, and Mei-M7 (KS-AT-DH-ER-KR-ACP) contains full reductive domains DH-ER-KR (He et al., 2010). If Mei-LM and Mei-M7 are assembled with TE domain (termed Mei-TE), the newly designed PKS (termed Mei-PKS) is expected to produce 2-methylbutyrate (Figure 1). If Mei-PKS is introduced into *S. avermitilis*, its product 2-methylbutyrate will be converted to MBCoA by acyl-CoA synthetase (ACS). AVE B1a production may therefore be enhanced as a result of increased MBCoA precursor level in cells.

To test our design, we amplified DNA fragments *mei-LM*, *mei-M7*, and *mei-TE* (respectively encoding Mei-LM, Mei-M7, and Mei-TE) from *S. nanchangensis* NS3226, and assembled them to generate *mei-pks*. *kasOp<sup>\*</sup>* is *Streptomyces* high-efficiency constitutive promoter displaying stronger activity than *ermEp<sup>\*</sup>* in *S. avermitilis* (Wang et al., 2013) and *aveBIIIp* is *S. avermitilis* native temporal promoter located within AVE biosynthetic gene cluster (Hao et al., 2022). In our previous study, B1a titer was effectively increased by *aveC8m* (an *aveC* variant) overexpression controlled by *kasOp<sup>\*</sup>* or *aveBIIIp* (Hao et al., 2022). Therefore, *mei-pks* was placed under control of *kasOp<sup>\*</sup>* or *aveBIIIp* for expression of engineered Mei-PKS. *kasOp<sup>\*</sup>-mei-pks* and *aveBIIIp-me-i-pks* were cloned separately into integrative plasmid pJ10500 (containing hygromycin resistance gene) (Pullan et al., 2011) to generate plasmids *pkasOp<sup>\*</sup>-mei-pks* and *paveBIIIp-me-i-pks*, which were separately transformed into *S. avermitilis* WT strain ATCC31267. Heterologous expression of *mei-pks* in *S. avermitilis* was assayed by RT-qPCR using RNA samples extracted from WT and the resulting transformants *kasOp<sup>\*</sup>-mei-pks* and *aveBIIIp-me-i-pks* grown in FM-I for 2, 4, 6, 8, or 10 days. Transcription of *mei-LM*, *mei-M7*, and *mei-TE* was detectable in *kasOp<sup>\*</sup>-mei-pks* and *aveBIIIp-me-i-pks*, but not in WT (Figure 2). Their levels were much higher in *kasOp<sup>\*</sup>-mei-pks* than in *aveBIIIp-me-i-pks* at various time points, demonstrating successful expression of *mei-pks* in *kasOp<sup>\*</sup>-mei-pks* and *aveBIIIp-me-i-pks*. These findings indicate that the activity of promoter *kasOp<sup>\*</sup>* is much stronger than that of *aveBIIIp*.

The two *mei-pks* expression strains did not display notable phenotypic differences from WT grown on YMS plates (Figure 3A), and biomass (dry cell weight) values of the two strains were similar to that of WT grown in soluble FM-II (Figure 3B). HPLC analysis of B1a titer from FM-I fermentation broth revealed strong enhancement of B1a production by *mei-pks* heterologous expression,

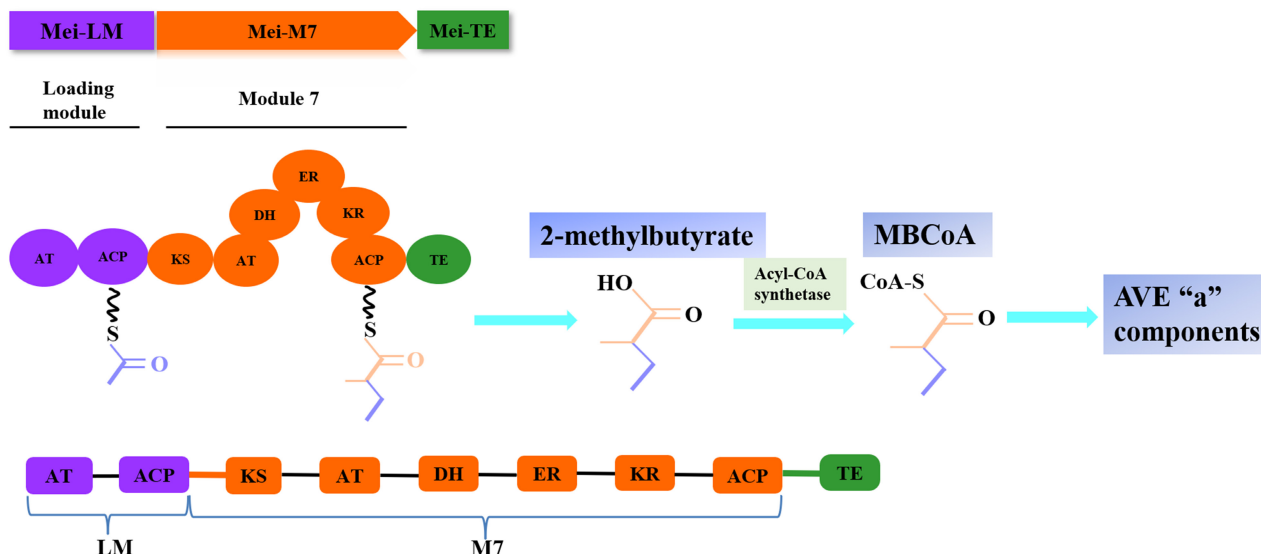


**FIGURE 1** Strategy for engineered Mei-PKS for 2-methylbutyrate production. The Mei-PKS contains MEI PKS loading module (LM) (using AcCoA as substrate), extension module 7 (M7) (using MMCoA as substrate), and TE domain. ACP, acyl carrier protein; AT, acyltransferase; CoA, coenzyme A; DH, dehydratase; ER, enoylreductase; KR, ketoreductase; KS, ketosynthase; MBCoA, 2-methylbutyryl-CoA.

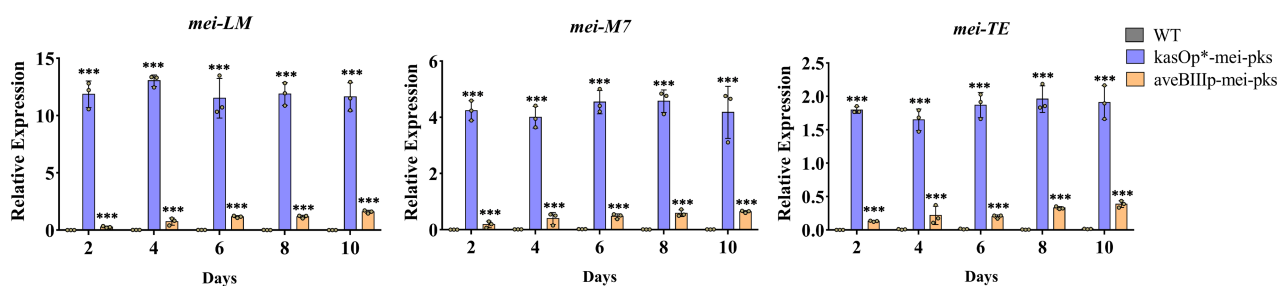


**FIGURE 2** RT-qPCR analysis of *mei-LM*, *mei-M7*, and *mei-TE*. RNA samples were isolated from WT, *kasOp\*-mei-pks*, and *aveBIIIp-me-pks* strains cultured in FM-I for 2, 4, 6, 8, or 10 days. \*\*\* $p < 0.001$  for comparison with WT (Student's *t*-test). Error bars: SD from three replicates.

and *kasOp\**-driven expression had a stronger promoting effect than did *aveBIIIp*-driven expression (Figure 3C). Final (day 10) B1a titer was 262.2  $\mu\text{g}/\text{mL}$  for *kasOp\*-mei-pks* (~4.36-fold higher than WT titer 48.9  $\mu\text{g}/\text{mL}$ ), and 239.9  $\mu\text{g}/\text{mL}$  for *aveBIIIp-me-pks* (~3.90-fold higher than WT) (Figure 3D, Figure S1). Heterologous expression of *mei-pks* in *S. avermitilis* is clearly an efficient strategy for enhancement of B1a production.

To investigate whether introduction of engineered Mei-PKS in *S. avermitilis* increases supply of MBCoA precursor for B1a production, we measured MBCoA levels in WT, *kasOp\*-mei-pks*, and *aveBIIIp-me-pks* strains cultured in FM-I for 2, 4, 6, and 8 days. On days 2 and 4, MBCoA levels were higher in *kasOp\*-mei-pks* than in *aveBIIIp-me-pks*, and higher in both these strains than in WT (Figure 3E), consistent with B1a titer data. In contrast, MBCoA levels on days 6 and 8 were similar for all three strains (Figure 3E). These findings indicate that Mei-PKS introduction leads to increased MBCoA precursor level in early and middle fermentation stages, and consequent promotion of B1a production.

## Downregulation of key FA synthesis pathway genes promotes B1a production

Each AVE PKS requires seven MalCoA extender units, which are derived mainly from carboxylation of AcCoA by AcCoA carboxylase. FA synthesis also requires AcCoA and MalCoA units. Thus, AVE biosynthesis competes with FA synthesis for common precursors. 3-oxoacyl-ACP synthase (encoded by *fabH*) and MalCoA:ACP transacylase (encoded by *fabD*) are essential enzymes controlling entry of AcCoA and MalCoA into FA synthesis pathway (Figure 4A). In *S. avermitilis*, four *fabH* genes [*fabH1* (*sav\_5787*), *fabH2* (*sav\_1831*), *fabH3* (*sav\_2290*), *fabH4* (*sav\_609*)], and one *fabD* gene (*sav\_5788*) were predicted to control these two key nodes (*S. avermitilis* KEGG database; <http://avermittils.ls.kitasato-u.ac.jp/kegg.html>). To increase MalCoA supply for AVE biosynthesis, we downregulated each of the above genes by CRISPRi using *S. avermitilis* native temporal promoter *pkn5p* (active mainly in middle and late fermentation stages) (Hao et al., 2022) and *E. coli*

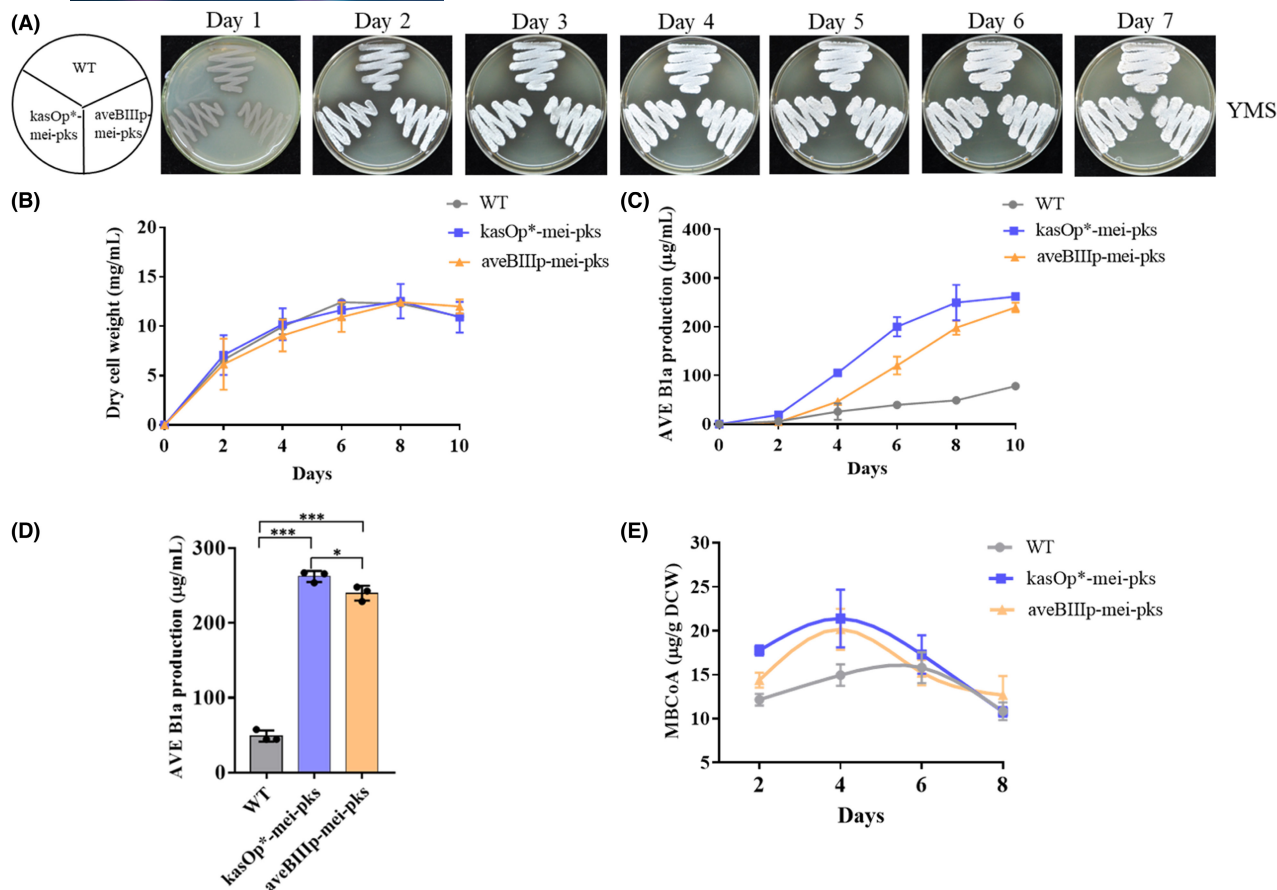


**FIGURE 3** Effects of introduction of *mei-pks* into *S. avermitilis* WT on phenotype, cell growth, B1a production, and MBCoA level. (A) Phenotypes of WT, *kasOp\**-*mei-pks*, and *aveBIIIp*-*mei-pks* grown on YMS plates at 28°C. (B) Growth curves of the three strains cultured in FM-II. Biomass is presented as dry cell weight. (C) Time course of B1a titer for the three strains cultured in FM-I. (D) B1a titers for the three strains on day 10. \* $p < 0.05$ ; \*\*\* $p < 0.001$  (*t*-test). (E) MBCoA levels for the three strains on days 2, 4, 6, and 8. MBCoA level is presented as µg per g dry cell weight (DCW). Error bars (panels B–E): SD from three replicates.

constitutive promoter *j23119p* (Larson et al., 2013) for expression of *dcas9* and sgRNA, respectively. *j23119p* has been verified as a strong promoter in model strain *S. coelicolor* (Zhao et al., 2018). One sgRNA was designed to target the NT strand of each gene coding region close to the start codon. Accordingly, five CRISPRi plasmids (*pfabH1<sup>i</sup>*, *pfabH2<sup>i</sup>*, *pfabH3<sup>i</sup>*, *pfabH4<sup>i</sup>*, *pfabD<sup>i</sup>*) were constructed and transformed separately into *S. avermitilis* WT strain, resulting in CRISPRi strains *fabH1<sup>i</sup>*, *fabH2<sup>i</sup>*, *fabH3<sup>i</sup>*, *fabH4<sup>i</sup>*, and *fabD<sup>i</sup>*. pSET-pkn5p-*dcas9* without 20-nt specific guide sequence ( $N_{20}$ ) of sgRNA was transformed into WT to generate plasmid control strain WT/*dcas9*. Transcription levels of the five *fab* genes were downregulated in corresponding CRISPRi strains, relative to levels in WT and WT/*dcas9*, particularly in middle and late fermentation stages (Figure 4B), consistent with *pkn5p* activity profile (Hao et al., 2022). These findings demonstrate successful inhibition of these genes in CRISPRi strains.

Analysis of final B1a titers in FM-I cultures revealed that transformation of pSET-pkn5p-*dcas9* into WT (strain WT/*dcas9*) had no effect on B1a titer, whereas inhibition of *fabH1*, *fabH2*, *fabH3*, *fabH4*, and *fabD*

(strains *fabH1<sup>i</sup>*, *fabH2<sup>i</sup>*, *fabH3<sup>i</sup>*, *fabH4<sup>i</sup>*, and *fabD<sup>i</sup>*) resulted in significantly increased B1a titers (Figure 4C, Figure S2). Strain *fabH2<sup>i</sup>* showed the highest B1a titer: 217.7 µg/mL, ~3.45-fold higher than WT and WT/*dcas9* values. Strain *fabD<sup>i</sup>* had the second highest B1a titer: 204.4 µg/mL, ~3.17-fold higher than WT and WT/*dcas9* values (Figure 4C). *fabH2* and *fabD* inhibition did not notably affect phenotype or cell growth (Figure S3A,B), but they increased MalCoA level, mainly in middle and late fermentation stages (Figure 4D). These findings indicate that *fabH* or *fabD* inhibition effectively enhances B1a production by increasing MalCoA precursor supply.

### Downregulation of key TCA cycle genes also promotes B1a production

Each AVE PKS also requires five MMCoA extender units. In TCA cycle, intermediate succinyl-CoA (SucCoA) is converted to succinate by SucCoA synthetase complex, which consists of  $\alpha$  and  $\beta$  subunits encoded respectively by genes *sucD* and *sucC* (Figure 5A). SucCoA can also

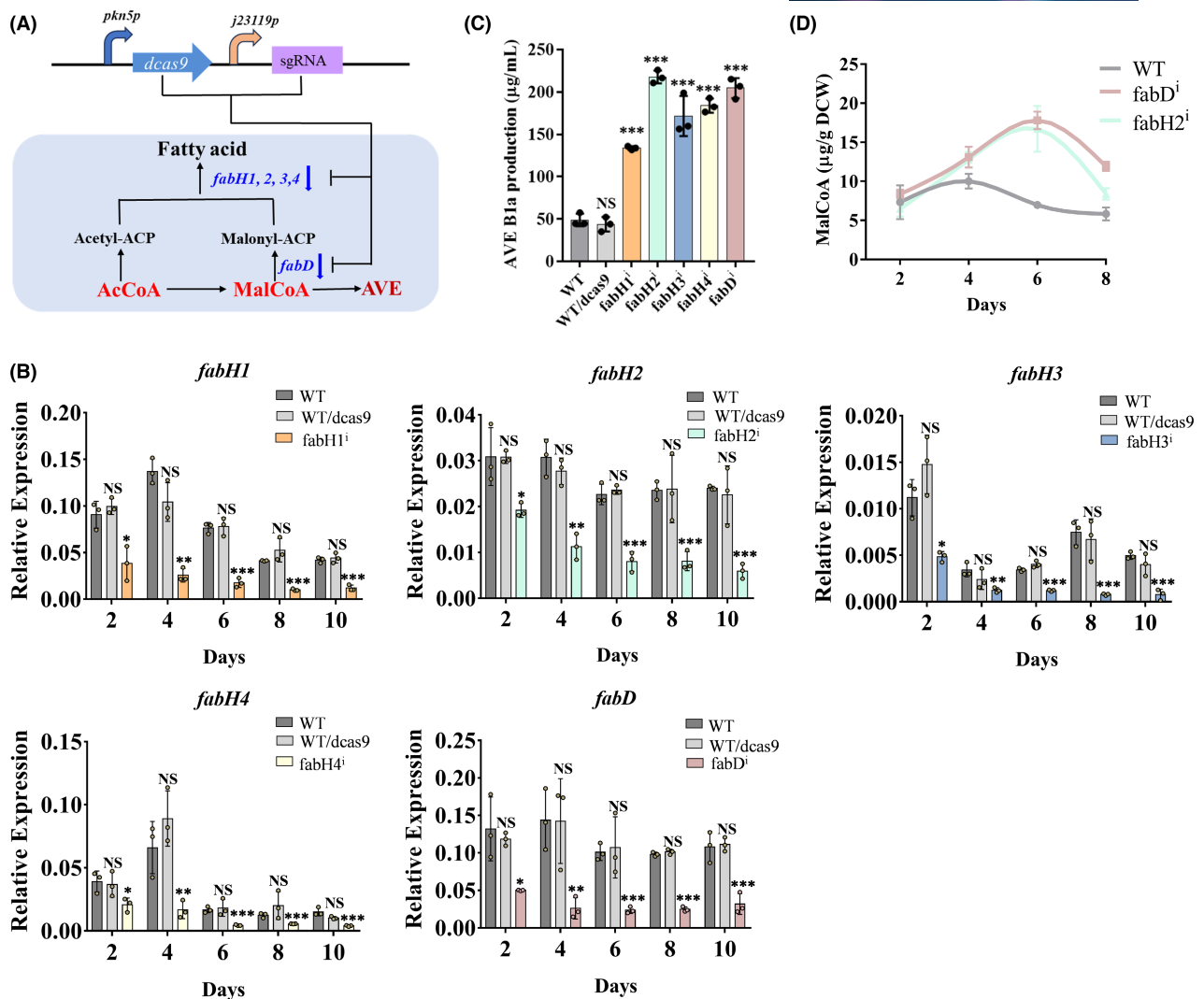


**FIGURE 4** Effects of inhibition of FA synthesis pathway genes *fabH* and *fabD* on B1a production in WT. (A) Relationship between FA synthesis pathway and AVE biosynthesis (schematic). Blue colour: two key nodes selected as CRISPRi targets. Each node involves one or four genes as indicated. (B) RT-qPCR analysis of *fabH1*, *fabH2*, *fabH3*, *fabH4*, and *fabD* in WT and corresponding CRISPRi strains cultured in FM-I. WT/*dcas9*: WT containing CRISPRi control plasmid pSET-*pkn5p*-*dcas9*. *fabH1*<sup>i</sup>, *fabH2*<sup>i</sup>, *fabH3*<sup>i</sup>, *fabH4*<sup>i</sup>, and *fabD*<sup>i</sup>: WT with CRISPRi-targeted *fabH1*, *fabH2*, *fabH3*, *fabH4*, and *fabD*. (C) B1a titers for WT and derived CRISPRi strains on day 10. (D) MalCoA levels for WT, *fabH2*<sup>i</sup>, and *fabD*<sup>i</sup>. Statistical notations (panels B, C): NS, not significant; \**p*<0.05; \*\**p*<0.01; \*\*\**p*<0.001 for comparison with WT (*t*-test). Error bars (panels B–D): SD from three replicates.

be converted to MMCoA by MMCoA mutase and MMCoA epimerase (Dayem et al., 2002). In *S. avermitilis*, two *sucC* genes [*sucC1* (*sav\_1818*), *sucC2* (*sav\_3452*)] and two *sucD* genes [*sucD1* (*sav\_1817*), *sucD2* (*sav\_3451*)] were predicted by *S. avermitilis* KEGG database to control this key node. To increase MMCoA supply for AVE biosynthesis, we inhibited gene pairs *sucC1D1* and *sucC2D2* for SucCoA synthetase complex in WT by CRISPRi, with the same strategy as for inhibition of *fab* genes. Successful inhibition of *sucC1D1* or *sucC2D2* in the resulting strains *sucC1D1*<sup>i</sup> or *sucC2D2*<sup>i</sup> was demonstrated by RT-qPCR analysis (Figure 5B).

Shake-flask fermentation results showed that final B1a titer was significantly increased by *sucC1D1* and *sucC2D2* inhibition. Titer for *sucC2D2*<sup>i</sup> (223.9 µg/mL)

was higher than for *sucC1D1*<sup>i</sup>, and ~3.57-fold higher than WT value (Figure 5C, Figure S4). Phenotype and cell growth did not differ notably between WT and *sucC2D2*<sup>i</sup> (Figure 5A,B), but MMCoA level was higher for *sucC2D2*<sup>i</sup> than for WT, mainly in middle and late fermentation stages (Figure 5D), and contributed to enhanced B1a production.

### Mei-PKS introduction combined with inhibition of three key nodes further promotes B1a production

To further increase B1a production, we inhibited *fabH2*, *fabD*, and *sucC2D2* singly or in combination in strain

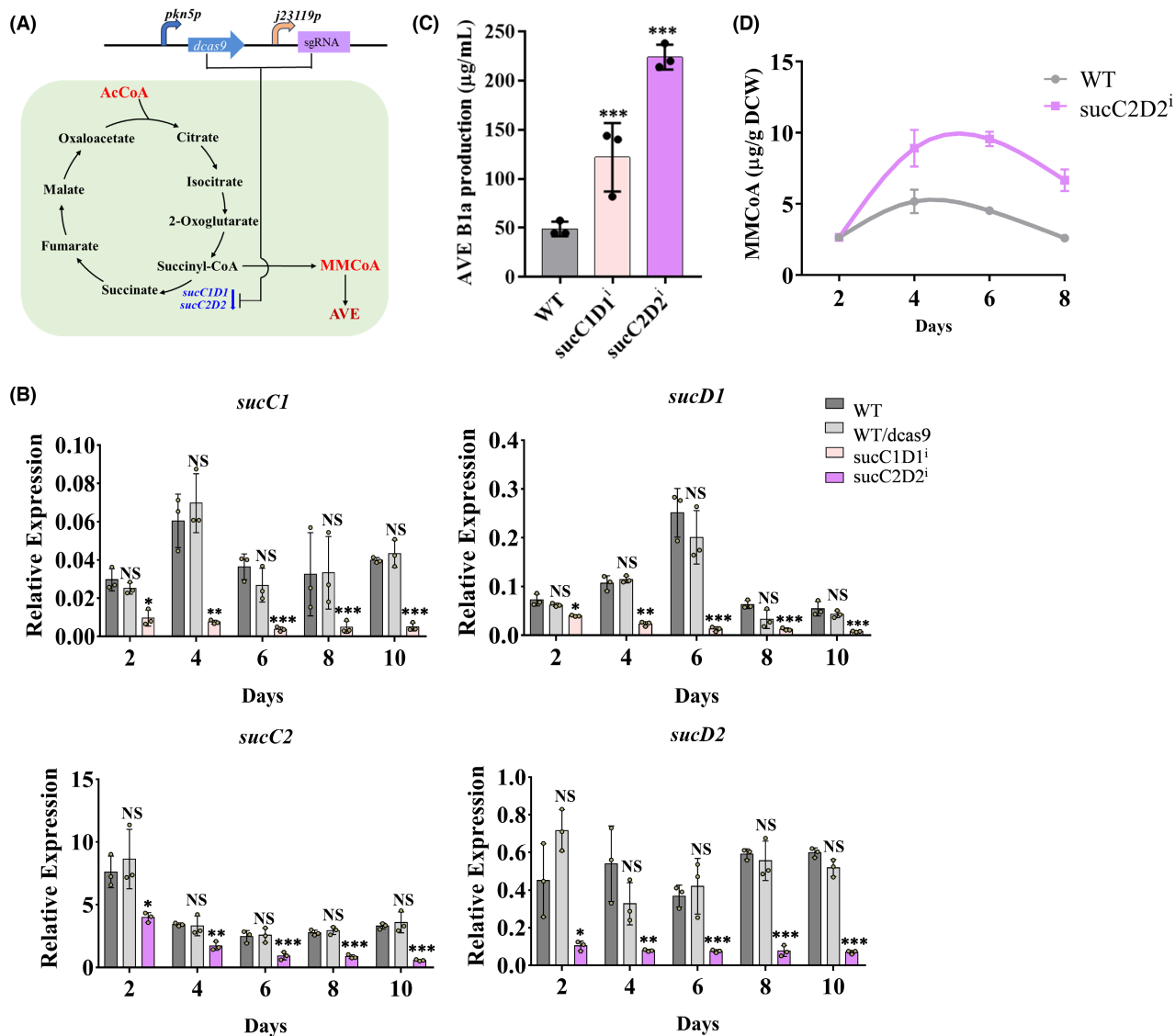


**FIGURE 5** Effects of inhibition of TCA cycle *sucCD* genes on B1a production in WT. (A) Relationship between TCA cycle pathway and AVE biosynthesis (schematic). Blue colour: two *sucCD* gene pairs selected as CRISPRi targets. (B) RT-qPCR analysis of *sucC1*, *sucD1*, *sucC2*, and *sucD2* in WT and corresponding CRISPRi strains cultured in FM-I. *sucC1D1<sup>i</sup>*: WT with CRISPRi-targeted *sucC1* and *sucD1*. *sucC2D2<sup>i</sup>*: WT with CRISPRi-targeted *sucC2* and *sucD2*. (C) B1a titers for WT, *sucC1D1<sup>i</sup>*, and *sucC2D2<sup>i</sup>* on day 10. (D) MMCoA levels for WT and *sucC2D2<sup>i</sup>*. Statistical notations as in Figure 4.

*kasOp<sup>\*</sup>-mei-pks*, generating six combination strains: *fabH2<sup>i</sup>-pks*, *fabD<sup>i</sup>-pks*, *sucC2D2<sup>i</sup>-pks*, *fabH2<sup>i</sup>sucC2D2<sup>i</sup>-pks*, *fabD<sup>i</sup>sucC2D2<sup>i</sup>-pks*, *fabH2<sup>i</sup>fabD<sup>i</sup>sucC2D2<sup>i</sup>-pks*. Each of the six strains showed final B1a titer higher than that of *kasOp<sup>\*</sup>-mei-pks*. *fabH2<sup>i</sup>fabD<sup>i</sup>sucC2D2<sup>i</sup>-pks* had the highest titer: 341.9 μg/mL, which was ~5.99-fold higher than WT value and ~30% higher than *kasOp<sup>\*</sup>-mei-pks* value (Figure 6, Figure S6). Phenotype and cell growth did not differ notably between *fabH2<sup>i</sup>fabD<sup>i</sup>sucC2D2<sup>i</sup>-pks* and WT (Figure S7A,B). These findings demonstrate that B1a production is effectively increased by combined engineering of MEI PKS and key nodes in FA synthesis and TCA cycle pathways.

## Effect of overexpression of β-oxidation pathway genes on B1a production

Conversion of 2-methylbutyrate (produced by Mei-PKS) to MBCoA requires ACS, an essential enzyme for activation of FAs by thioesterification with CoA for entry into β-oxidation cycle. In *S. avermitilis*, 22 genes were predicted to encode ACS. Wang et al. (2020) found that *S. coelicolor* ACS SCO6196 (*FadD1*), which is conserved in genus *Streptomyces*, displays substrate promiscuity and controls degradation of cellular TAG pool during stationary phase. Accordingly, they used ACS gene *sco6196* for construction of ddTAG module to control TAG degradation. The *S. avermitilis* gene

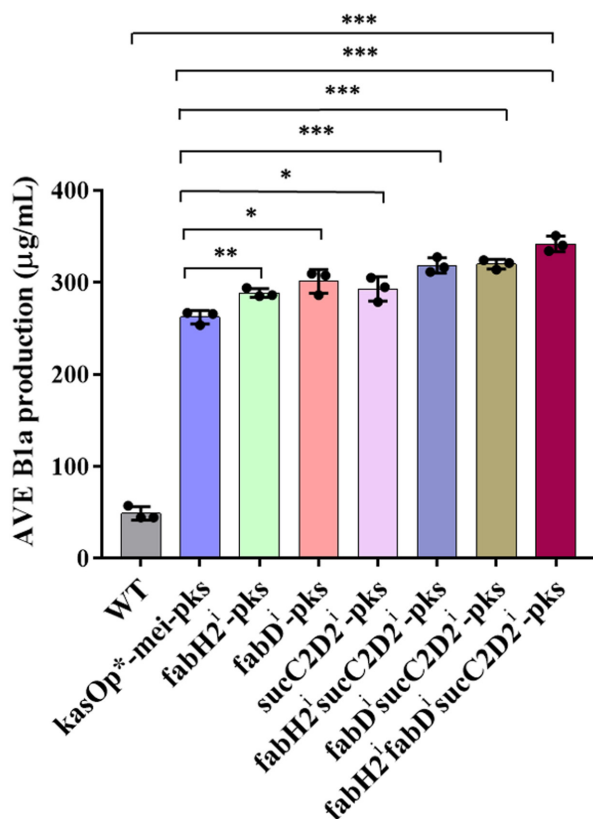


**FIGURE 6** Effects of inhibition of *fabH2*, *fabD*, or/and *sucC2D2* genes on B1a production in *kasOp\**-*mei*-*pks*. \* $p < 0.05$ ; \*\* $p < 0.01$ ; \*\*\* $p < 0.001$  for comparison with *kasOp\**-*mei*-*pks* or WT (*t*-test). Error bars: SD from three replicates.

homologous to *sco6196* is *sav\_2030* (termed *fadD*). We observed previously that overexpression of *fadD* and/or  $\beta$ -oxidation pathway gene pair *fadAB* (corresponding to *sav\_2233*, *sav\_2234*) in *S. avermitilis* increased levels of MalCoA and MMCoA precursors for AVE biosynthesis and thereby enhanced B1a production (Hao et al., 2022). Based on this finding, we co-overexpressed *pkn5p*-driven *fadD* and *fadAB* in *kasOp\**-*mei*-*pks*, using multicopy plasmid pOfadD-*fadAB*. The resulting strain OfadD-*fadAB*-*pks* did not differ notably from WT in terms of phenotype or cell growth (Figure S8A,B), but had final B1a titer 339.7  $\mu\text{g/mL}$  – 29.5% higher than that of *kasOp\**-*mei*-*pks* (Figure 7A, Figure S9). This co-overexpression of *fadD* and *fadAB* further increased MBCoA level in addition to increasing MalCoA and MMCoA levels on days 6 and 8 (Figure 7B), accounting for the further increase of B1a titer.

Possible integrative effect was investigated by co-overexpressing *fadD* and *fadAB* in recombinant strain *fabH2<sup>i</sup>fabD<sup>i</sup>sucC2D2<sup>i</sup>-pks*. This strain carries CRISPRi plasmids constructed using integrative plasmid pSET152, which contains apramycin resistance gene *aac(3)/IV*. *fadD*-*fadAB* co-overexpressing plasmid pOfadD-*fadAB* (Hao et al., 2022) was constructed using multicopy plasmid *pKC1139*, which

also contains *aac(3)/IV*. It was not possible to directly transform pOfadD-*fadAB* into *fabH2<sup>i</sup>fabD<sup>i</sup>sucC2D2<sup>i</sup>-pks*. Moreover, *pKC1139* is a multicopy plasmid that is unstable without antibiotic selection and is not suitable for industrial production. We therefore amplified *pkn5p*-*fadD*-*fadAB* fragment from plasmid pOfadD-*fadAB* and ligated it into CRISPRi plasmid *pfabH2<sup>i</sup>fabD<sup>i</sup>sucC2D2<sup>i</sup>* to generate pOfad-*fabH2<sup>i</sup>fabD<sup>i</sup>sucC2D2<sup>i</sup>*, which was then transformed into *kasOp\**-*mei*-*pks*. The resulting strain Ofad-*fab<sup>i</sup>suc<sup>i</sup>-pks* was similar to WT in terms of phenotype and cell growth (Figure S8A,B), but had final B1a titer 452.8  $\mu\text{g/mL}$  – respectively 72.6%, 33.3%, and 32.4% higher than values for *kasOp\**-*mei*-*pks*, OfadD-*fadAB*-*pks*, and *fabH2<sup>i</sup>fabD<sup>i</sup>sucC2D2<sup>i</sup>-pks* (Figure 7A, Figure S9).

In summary, a combination strategy for enhancement of MBCoA, MalCoA, and MMCoA levels involving heterologous expression of *Mei*-PKS, inhibition of key nodes in FA synthesis and TCA cycle pathways, and co-overexpression of  $\beta$ -oxidation pathway genes *fadD* and *fadAB* resulted in greatly increased B1a titer 452.8  $\mu\text{g/mL}$ , which was ~8.25-fold higher than WT value (Figure 7A).

### Acyl-CoA precursor supply strategies increase B1a production in industrial strain

In view of the greatly increased B1a production in WT strain achieved using the above-described acyl-CoA precursor supply strategies, we experimentally applied these strategies in industrial strain A229. Plasmid *pkasOp\**-*mei*-*pks* was transformed into A229 to generate strain *kasOp\**-*mei*-*pks*/A229. Final B1a titer for *kasOp\**-*mei*-*pks*/A229 was 7252.4  $\mu\text{g/mL}$  – 13% higher than the value (6411.7  $\mu\text{g/mL}$ ) for parental A229 (Figure 8, Figure S10). We investigated possible combination strategy by separately transforming *pfabH2<sup>i</sup>fabD<sup>i</sup>sucC2D2<sup>i</sup>* and pOfad-*fabH2<sup>i</sup>fabD<sup>i</sup>sucC2D2<sup>i</sup>* into *kasOp\**-*mei*-*pks*/A229 to generate strains *fabH2<sup>i</sup>fabD<sup>i</sup>sucC2D2<sup>i</sup>-pks*/A229 and Ofad-*fab<sup>i</sup>suc<sup>i</sup>-pks*/A229. Final B1a titers for these two strains were respectively 7717.8 and 8836.4  $\mu\text{g/mL}$  – 20.3% and 37.8% higher than A229 value (Figure 8, Figure S10). We conclude that our acyl-CoA precursor supply strategies effectively enhance B1a production in industrial strain.

## DISCUSSION

During *Streptomyces* fermentation, polyketides are synthesized mainly during stationary phase. Polyketide production is typically limited by availability of acyl-CoA precursors because they are required for cell growth and are generated by primary

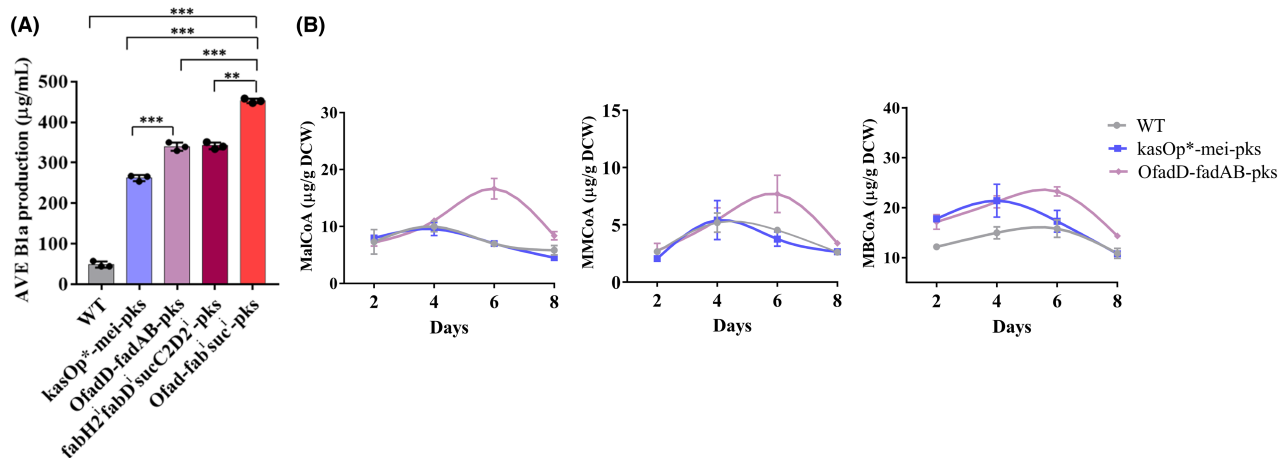


**FIGURE 7** Effects of combination of acyl-CoA precursor supply strategies on B1a production in WT. (A) B1a titers for WT, kasOp<sup>\*</sup>-mei-pks, OfadD-fadAB-pks (kasOp<sup>\*</sup>-mei-pks with plasmid pOfadD-fadAB), fabH2<sup>Δ</sup>fabD<sup>Δ</sup>sucC2D2<sup>Δ</sup>-pks (kasOp<sup>\*</sup>-mei-pks with CRISPRi-targeted *fabH2*, *fabD*, *sucC2*, and *sucD2*), and Ofad-fab<sup>Δ</sup>suc<sup>Δ</sup>-pks (kasOp<sup>\*</sup>-mei-pks with *pkn5p-fadD-fadAB* and CRISPRi-targeted *fabH2*, *fabD*, *sucC2*, and *sucD2*) on day 10 of FM-I culture. (B) MalCoA, MMCoA, and MBCoA levels for WT, kasOp<sup>\*</sup>-mei-pks, and OfadD-fadAB-pks. \*\**p* < 0.01; \*\*\**p* < 0.001 (*t*-test). Error bars: SD from three replicates.

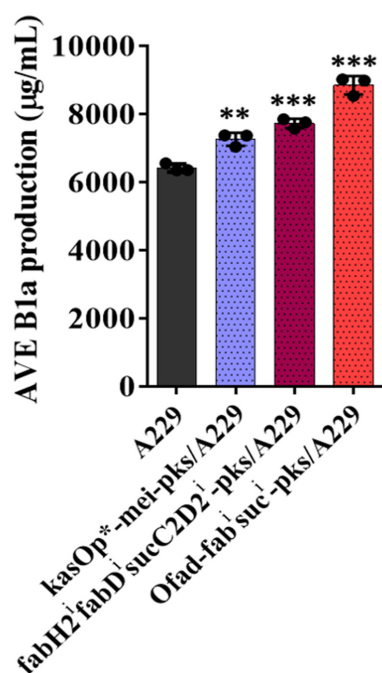


**FIGURE 8** Effects of combination of acyl-CoA precursor supply strategies on B1a production in industrial strain A229. kasOp<sup>\*</sup>-mei-pks/A229: A229 with plasmid pkasOp<sup>\*</sup>-mei-pks. fabH2<sup>Δ</sup>fabD<sup>Δ</sup>sucC2D2<sup>Δ</sup>-pks/A229: kasOp<sup>\*</sup>-mei-pks/A229 with CRISPRi-targeted *fabH2*, *fabD*, *sucC2*, and *sucD2*. Ofad-fab<sup>Δ</sup>suc<sup>Δ</sup>-pks/A229: kasOp<sup>\*</sup>-mei-pks/A229 with *pkn5p-fadD-fadAB* and CRISPRi-targeted *fabH2*, *fabD*, *sucC2*, and *sucD2*. \*\**p* < 0.01; \*\*\**p* < 0.001 for comparison with A229 (*t*-test). Error bars: SD for three replicates.

metabolism, which declines during stationary phase. Increased supply of acyl-CoA precursors is therefore necessary for increased polyketide production

(Li et al., 2021). MBCoA is used as starter unit for synthesis of AVE “a” components and is evidently isoleucine-derived based on feeding studies (Ikeda & Omura, 1997). However, B1a production was not increased by overexpression of isoleucine biosynthesis genes (our unpublished data). In the present study, we enhanced MBCoA precursor supply by heterologous expression of newly designed Mei-PKS, and thereby greatly increased B1a titer in *S. avermitilis* WT and industrial strains. The engineered Mei-PKS effectively enhanced MBCoA level and is presumably applicable in other industrial *Streptomyces* species that require MBCoA precursor for polyketide production. More generally, approaches described here can be applied to enhance levels of unusual acyl-CoAs based on rational construction of hybrid PKSs.

We used two promoters (*kasOp<sup>\*</sup>*, *aveBIIIp*) to express *mei-pks* for Mei-PKS in *S. avermitilis*. Transcription level of constitutive strong promoter *kasOp<sup>\*</sup>*-driven *mei-pks* was shown by RT-qPCR analysis to be ~2.5- to 9.3-fold higher than that of native temporal promoter *aveBIIIp*-driven *mei-pks* at various time points. However, final B1a titer for strain kasOp<sup>\*</sup>-mei-pks was only 9.2% higher than that for *aveBIIIp*-mei-pks, indicating that *mei-pks* expression level was not precisely proportional to B1a titer. Although B1a titer was more effectively increased by *kasOp<sup>\*</sup>*-driven *mei-pks* than by *aveBIIIp*-driven *mei-pks*, *kasOp<sup>\*</sup>* may be not optimal for B1a production; B1a titer may be further increased using *mei-pks* driven by certain strong native temporal promoters. To this end, cellobiose-inducible (Wang et al., 2021) and cumate-inducible promoters (Hou et al., 2018) can be used to “fine-tune” *mei-pks* expression based on addition

of differing inducer dosages at different fermentation time points, which can optimize induction conditions for B1a production in both time and strength dimensions (Li et al., 2017). Accordingly, *S. avermitilis* native promoters with transcription behaviours similar to that of inducible promoter under optimal condition can be used for *mei-pks* expression, resulting in optimal B1a production with no need for inducers. Systematic identification of *S. avermitilis* native temporal promoters in future studies is an urgent requirement to facilitate optimization of B1a production through metabolic engineering and synthetic biological methods.

In addition to B1a titer, engineered Mei-PKS also increased B1b titer, and B1a: B1b ratios for strains *kasOp\**-*mei-pks* and *aveBIIIp*-*mei-pks* were similar to that for WT (Figures S1 and S11), perhaps as a result of substrate miscibility in our extension module. IsoBuCoA is the required starter unit for biosynthesis of AVE “b” components. One possibility is that AT domain of Mei-M7 can also incorporate MalCoA as extender unit, leading to less amount of butyrate production by engineered Mei-PKS. Butyryl-CoA, the activated form of butyrate, can be converted to IsoBuCoA by a coenzyme B12-dependent IsoBuCoA mutase (Chan et al., 2009; Vrijbloed et al., 1999), providing the starter unit for B1b production. This possibility was supported by our finding that IsoBuCoA levels were higher in strains *kasOp\**-*mei-pks* and *aveBIIIp*-*mei-pks* than in WT on days 2 and 4 of FM-I culture (Figure S12), consistent with MBCoA level data. The mechanism whereby B1b titer is enhanced by Mei-PKS remains to be elucidated.

AVE biosynthesis requires MalCoA and MMCoA as extender units. MalCoA and its precursor AcCoA are also required for FA synthesis. SucCoA in TCA cycle can be converted to MMCoA. To increase MalCoA and MMCoA supplies and B1a titer, we therefore selected two key nodes (*fabH* and *fabD*, controlling entry of AcCoA and MalCoA) in FA synthesis pathway and one key node (*sucCD*, controlling conversion of SucCoA to succinate) in TCA cycle pathway for CRISPRi. *S. avermitilis* KEGG database indicates that *fabD* is presented by one gene, *fabH* by four genes (*fabH1*, *fabH2*, *fabH3*, *fabH4*), and *sucCD* by two gene pairs (*sucC1D1*, *sucC2D2*). Each of the key nodes we selected is involved in an essential cellular pathway, and inhibition of the above genes may therefore result in cell growth arrest. Gao et al. (2021) constructed a CRISPRi circuit for autonomous control of metabolic flux in *E. coli* by designing sgRNA expressed by a stationary phase promoter. To avoid CRISPRi-mediated inhibition of selected key nodes affecting cell growth, we used *S. avermitilis* native temporal promoter *pkn5p* (active mainly in middle and late fermentation stages) (Hao et al., 2022) to regulate *dcas9* expression. Separate inhibition of genes for each of these key nodes in WT strongly increased B1a titer. For *fabH* and *sucCD* nodes, inhibition

of *fabH2* and *sucC2D2* had the strongest enhancing effect on B1a titer. Inhibition of *fabH2*, *fabD*, or *sucC2D2* did not notably affect phenotype and cell growth, but did increase MalCoA or MMCoA levels, mainly in middle and late fermentation stages. B1a titer was more strongly increased by combined inhibition (in comparison with separate inhibition) of *fabH2*, *fabD*, and *sucC2D2* in *kasOp\**-*mei-pks*. These findings indicate that inhibition of *fabH*, *fabD*, and *sucCD* genes in middle and late fermentation stages is an effective strategy for increasing levels of MalCoA and MMCoA precursors and thereby enhancing B1a production.

We selected only one TCA cycle pathway node (*sucCD*) for CRISPRi. Citrate synthase (GltA) catalyses formation of citrate from AcCoA and oxaloacetate, which is the first step of the cycle and involves AcCoA consumption. GltA is therefore located at the key node of TCA cycle and polyketide synthesis pathways. Liu et al. (2021) reported that CRISPRi-mediated inhibition of *gltA* in *S. bingchenggensis* weakened TCA cycle, and increased AcCoA level and milbemycin production. Possible enhancement of B1a production in *S. avermitilis* by *gltA* inhibition is the subject of current studies. Essential pathways other than TCA cycle and FA synthesis pathways, for example, pentose phosphate and glycolysis pathways, may also be modulated by CRISPRi to redirect metabolic flux towards AVE synthesis. B1a titer may also be further enhanced through design of additional sgRNAs for key node genes, and optimization of gene inhibition strengths.

Activation of Mei-PKS-generated 2-methylbutyrate to MBCoA requires ACS, which is also required for activation of FAs through CoA thioesterification to enter  $\beta$ -oxidation cycle. We found previously that overexpression of ACS gene *fadD* (*sav\_2030*) and  $\beta$ -oxidation pathway gene pair *fadAB* (*sav\_2233*, *sav\_2234*) in *S. avermitilis* increased MalCoA and MMCoA supplies and B1a titer (Hao et al., 2022). Accordingly, we co-overexpressed *fadD* and *fadAB* in *kasOp\**-*mei-pks*, and observed increased B1a titer in the resulting strain *OfadD-fadAB-pks*. MBCoA level was higher in *OfadD-fadAB-pks* than in *kasOp\**-*mei-pks*, indicating that *fadD* gene product is also useful for activation of 2-methylbutyrate. Combination of our acyl-CoA precursor supply strategies in industrial strain A229 resulted in B1a titer 8836.4  $\mu\text{g}/\text{mL}$ . 8 *fadA* genes, 2 *fadB* genes, and 17 putative *fadD* genes are present in *S. avermitilis* genome, and their specific functions have not yet been characterized. Combinatorial overexpression of these *fad* genes may optimize candidate genes and make possible further enhancement of B1a titer.

In summary, we achieved significant increase of AVE B1a titer in *S. avermitilis* WT and industrial strains by enhancing supplies of both acyl-CoA starter and extender units for B1a synthesis (Figure 9). Such

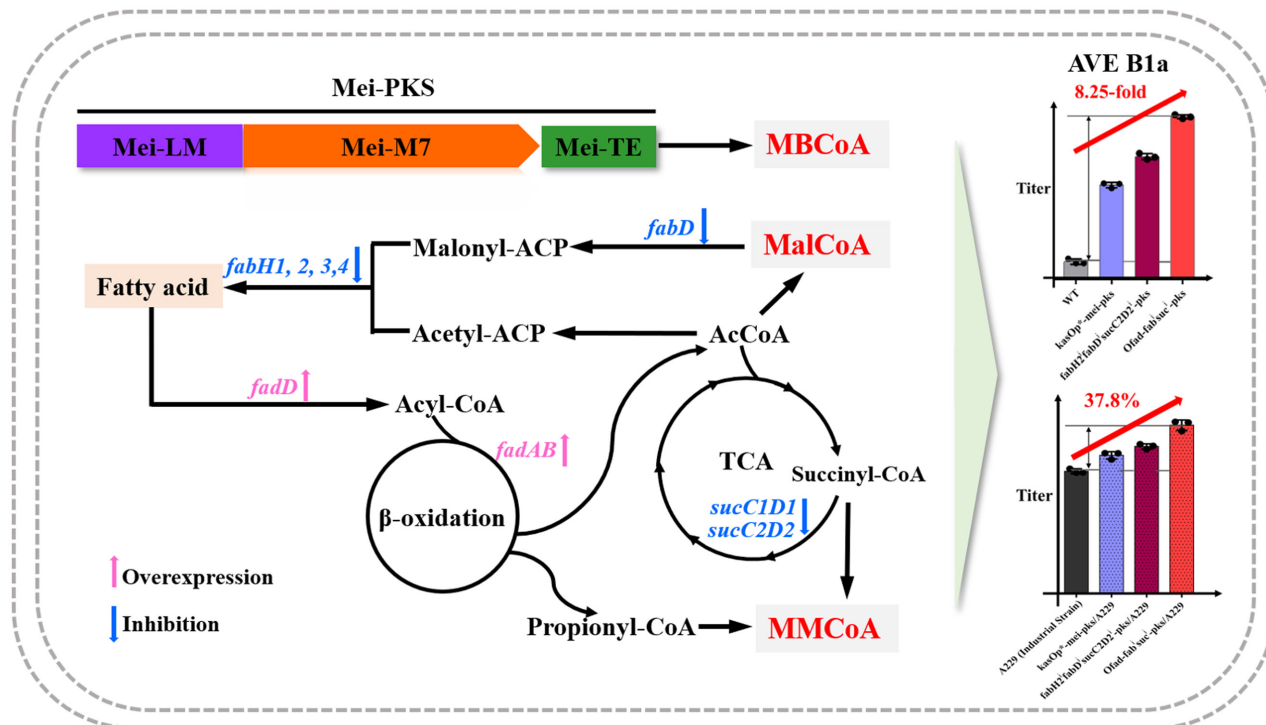


**FIGURE 9** Strategies for enhanced acyl-CoA precursor supply for high B1a production. AcCoA, acetyl-CoA; MalCoA, malonyl-CoA; MBCoA, 2-methylbutyryl-CoA; MMCoA, methylmalonyl-CoA.

precursor supply strategies can be readily adapted for overproduction of other polyketides.

## AUTHOR CONTRIBUTIONS

**Mengyao Yang:** Data curation; formal analysis; investigation; validation; visualization; writing – original draft. **Yi Hao:** Data curation; validation; visualization. **Gang Liu:** Funding acquisition; supervision. **Ying Wen:** Conceptualization; funding acquisition; resources; supervision; writing – original draft; writing – review and editing.

## ACKNOWLEDGEMENTS

The authors are grateful to prof. Linquan Bai (Shanghai Jiao Tong University, Shanghai, China) for providing *S. nanchangensis* NS3226, and to Dr. S. Anderson for English editing of the manuscript.

## FUNDING INFORMATION

This study was supported by the National Key Research and Development Program of China (grants no. 2021YFC2100600 and 2023YFC3402400).

## CONFLICT OF INTEREST STATEMENT

The authors declare no conflicts of interest.

## DATA AVAILABILITY STATEMENT

The data is presented in the manuscript.

## ORCID

Gang Liu  <https://orcid.org/0000-0003-3583-2985>

Ying Wen  <https://orcid.org/0000-0001-8455-6900>

## REFERENCES

- Barajas, J.F., Blake-Hedges, J.M., Bailey, C.B., Curran, S. & Keasling, J.D. (2017) Engineered polyketides: synergy between protein and host level engineering. *Synthetic and Systems Biotechnology*, 2, 147–166.
- Blin, K., Pedersen, L.E., Weber, T. & Lee, S.Y. (2016) CRISPy-web: an online resource to design sgRNAs for CRISPR applications. *Synthetic and Systems Biotechnology*, 1, 118–121.
- Burg, R.W., Miller, B.M., Baker, E.E., Birnbaum, J., Currie, S.A., Hartman, R. et al. (1979) Avermectins, new family of potent anthelmintic agents: producing organism and fermentation. *Antimicrobial Agents and Chemotherapy*, 15, 361–367.
- Cao, Z., Yu, J., Wang, W., Lu, H., Xia, X., Xu, H. et al. (2020) Multi-scale data-driven engineering for biosynthetic titer improvement. *Current Opinion in Biotechnology*, 65, 205–212.
- Chan, Y.A., Podevels, A.M., Kevany, B.M. & Thomas, M.G. (2009) Biosynthesis of polyketide synthase extender units. *Natural Product Reports*, 26, 90–114.
- Dayem, L.C., Carney, J.R., Santi, D.V., Pfeifer, B.A., Khosla, C. & Kealey, J.T. (2002) Metabolic engineering of a methylmalonyl-CoA mutase-epimerase pathway for complex polyketide biosynthesis in *Escherichia coli*. *Biochemistry*, 41, 5193–5201.
- Deng, Q., Xiao, L., Liu, Y., Zhang, L., Deng, Z. & Zhao, C. (2019) *Streptomyces avermitilis* industrial strain as cell factory for Ivermectin B1a production. *Synthetic and Systems Biotechnology*, 4, 34–39.
- Egerton, J.R., Ostlind, D.A., Blair, L.S., Eary, C.H., Suhayda, D., Cifelli, S. et al. (1979) Avermectins, new family of

- potent anthelmintic agents: efficacy of the B1a component. *Antimicrobial Agents and Chemotherapy*, 15, 372–378.
- El-Saber Batiha, G., Alqahtani, A., Ilesanmi, O.B., Saati, A.A., El-Mleeh, A., Hetta, H.F. et al. (2020) Avermectin derivatives, pharmacokinetics, therapeutic and toxic dosages, mechanism of action, and their biological effects. *Pharmaceuticals*, 13, 196.
- Gao, C., Guo, L., Hu, G., Liu, J., Chen, X., Xia, X. et al. (2021) Engineering a CRISPRi circuit for autonomous control of metabolic flux in *Escherichia coli*. *ACS Synthetic Biology*, 10, 2661–2671.
- Hagen, A., Poust, S., de Rond, T., Yuzawa, S., Katz, L., Adams, P.D. et al. (2014) In vitro analysis of carboxyacyl substrate tolerance in the loading and first extension modules of borrelidin polyketide synthase. *Biochemistry*, 53, 5975–5977.
- Hagen, A., Poust, S., Rond, T., Fortman, J.L., Katz, L., Petzold, C.J. et al. (2016) Engineering a polyketide synthase for in vitro production of adipic acid. *ACS Synthetic Biology*, 5, 21–27.
- Hao, Y., You, Y., Chen, Z., Li, J., Liu, G. & Wen, Y. (2022) Avermectin B1a production in *Streptomyces avermitilis* is enhanced by engineering aveC and precursor supply genes. *Applied Microbiology and Biotechnology*, 106, 2191–2205.
- He, Y., Sun, Y., Liu, T., Zhou, X., Bai, L. & Deng, Z. (2010) Cloning of separate meilingmycin biosynthesis gene clusters by use of acyltransferase-ketoreductase didomain PCR amplification. *Applied and Environmental Microbiology*, 76, 3283–3292.
- Hou, J., Zeng, W., Zong, Y., Chen, Z., Miao, C., Wang, B. et al. (2018) Engineering the ultrasensitive transcription factors by fusing a modular oligomerization domain. *ACS Synthetic Biology*, 7, 1188–1194.
- Ikeda, H., Kotaki, H., Tanaka, H. & Omura, S. (1988) Involvement of glucose catabolism in avermectin production by *Streptomyces avermitilis*. *Antimicrobial Agents and Chemotherapy*, 32, 282–284.
- Ikeda, H., Nonomiya, T. & Omura, S. (2001) Organization of biosynthetic gene cluster for avermectin in *Streptomyces avermitilis*: analysis of enzymatic domains in four polyketide synthases. *Journal of Microbiology and Biotechnology*, 27, 170–176.
- Ikeda, H., Nonomiya, T., Usami, M., Ohta, T. & Omura, S. (1999) Organization of the biosynthetic gene cluster for the polyketide anthelmintic macrolide avermectin in *Streptomyces avermitilis*. *Proceedings of the National Academy of Sciences of the United States of America*, 96, 9509–9514.
- Ikeda, H. & Omura, S. (1997) Avermectin biosynthesis. *Chemical Reviews*, 97, 2591–2609.
- Jiang, L., Liu, Y., Wang, P., Wen, Y., Song, Y., Chen, Z. et al. (2011) Inactivation of the extracytoplasmic function sigma factor Sig6 stimulates avermectin production in *Streptomyces avermitilis*. *Biotechnology Letters*, 33, 1955–1961.
- Jones, G., Del Sol, R., Dudley, E. & Dyson, P. (2011) Forkhead-associated proteins genetically linked to the serine/threonine kinase PknB regulate carbon flux towards antibiotic biosynthesis in *Streptomyces coelicolor*. *Microbial Biotechnology*, 4, 263–274.
- Kieser, T., Bibb, M.J., Buttner, M.J., Chater, K.F. & Hopwood, D.A. (2000) *Practical Streptomyces genetics: a laboratory manual*. Norwich, UK: John Innes Foundation.
- Kudo, K., Hashimoto, T., Hashimoto, J., Kozono, I., Kagaya, N., Ueoka, R. et al. (2020) In vitro Cas9-assisted editing of modular polyketide synthase genes to produce desired natural product derivatives. *Nature Communications*, 11, 4022.
- Larson, M.H., Gilbert, L.A., Wang, X., Lim, W.A., Weissman, J.S. & Qi, L.S. (2013) CRISPR interference (CRISPRi) for sequence-specific control of gene expression. *Nature Protocols*, 8, 2180–2196.
- Li, S., Li, Z., Pang, S., Xiang, W. & Wang, W. (2021) Coordinating precursor supply for pharmaceutical polyketide production in *Streptomyces*. *Current Opinion in Biotechnology*, 69, 26–34.
- Li, S., Wang, J., Xiang, W., Yang, K., Li, Z. & Wang, W. (2017) An autoregulated fine-tuning strategy for titer improvement of secondary metabolites using native promoters in *Streptomyces*. *ACS Synthetic Biology*, 7, 522–530.
- Liu, W., Zhang, Q., Guo, J., Chen, Z., Li, J. & Wen, Y. (2015) Increasing avermectin production in *Streptomyces avermitilis* by manipulating the expression of a novel tetR-family regulator and its target gene product. *Applied and Environmental Microbiology*, 81, 5157–5173.
- Liu, Y., Wang, H., Li, S., Zhang, Y., Cheng, X., Xiang, W. et al. (2021) Engineering of primary metabolic pathways for titer improvement of milbemycins in *Streptomyces bingchengensis*. *Applied Microbiology and Biotechnology*, 105, 1875–1887.
- Luo, S., Sun, D., Zhu, J., Chen, Z., Wen, Y. & Li, J. (2014) An extracytoplasmic function sigma factor,  $\sigma(25)$ , differentially regulates avermectin and oligomycin biosynthesis in *Streptomyces avermitilis*. *Applied Microbiology and Biotechnology*, 98, 7097–7112.
- Lyu, M., Cheng, Y., Han, X., Wen, Y., Song, Y., Li, J. et al. (2020) AccR, a tetR family transcriptional repressor, coordinates short-chain acyl coenzyme A homeostasis in *Streptomyces avermitilis*. *Applied and Environmental Microbiology*, 86, e00508-20.
- Macneil, D.J. & Klapko, L.M. (1987) Transformation of *Streptomyces avermitilis* by plasmid DNA. *Journal of Industrial Microbiology & Biotechnology*, 2, 209–218.
- Pullan, S.T., Chandra, G., Bibb, M.J. & Merrick, M. (2011) Genome-wide analysis of the role of GlnR in *Streptomyces venezuelae* provides new insights into global nitrogen regulation in actinomycetes. *BMC Genomics*, 12, 175.
- Rokem, J.S., Lantz, A.E. & Nielsen, J. (2007) Systems biology of antibiotic production by microorganisms. *Natural Product Reports*, 24, 1262–1287.
- Sun, Y., Zhou, X., Liu, J., Bao, K., Zhang, G., Tu, G. et al. (2002) '*Streptomyces nanchangensis*', a producer of the insecticidal polyether antibiotic nanchangmycin and the antiparasitic macrolide meilingmycin, contains multiple polyketide gene clusters. *Microbiology*, 148, 361–371.
- Tian, J., Yang, G., Gu, Y., Sun, X., Lu, Y. & Jiang, W. (2020) Developing an endogenous quorum-sensing based CRISPRi circuit for autonomous and tunable dynamic regulation of multiple targets in *Streptomyces*. *Nucleic Acids Research*, 48, 8188–8202.
- Vrijbloed, J.W., Zerbe-Burkhardt, K., Ratnatilleke, A., Grubelnik-Leiser, A. & Robinson, J.A. (1999) Insertional inactivation of methylmalonyl coenzyme A (CoA) mutase and isobutyryl-CoA mutase genes in *Streptomyces cinnamonensis*: influence on polyketide antibiotic biosynthesis. *Journal of Bacteriology*, 181, 5600–5605.
- Wang, W., Li, S., Li, Z., Zhang, J., Fan, K., Tan, G. et al. (2020) Harnessing the intracellular triacylglycerols for titer improvement of polyketides in *Streptomyces*. *Nature Biotechnology*, 38, 76–83.
- Wang, W., Li, X., Wang, J., Xiang, S., Feng, X. & Yang, K. (2013) An engineered strong promoter for *streptomycetes*. *Applied and Environmental Microbiology*, 79, 4484–4492.
- Wang, X., Fu, Y., Wang, M. & Niu, G. (2021) Synthetic cellobiose-inducible regulatory systems allow tight and dynamic controls of gene expression in *Streptomyces*. *ACS Synthetic Biology*, 10, 1956–1965.
- Yoon, Y.J., Kim, E.S., Hwang, Y.S. & Choi, C.Y. (2004) Avermectin: biochemical and molecular basis of its biosynthesis and regulation. *Applied Microbiology and Biotechnology*, 63, 626–634.

Yuzawa, S., Mirsiaghi, M., Jovic, R., Fujii, T., Masson, F., Benites, V.T. et al. (2018) Short-chain ketone production by engineered polyketide synthases in *Streptomyces albus*. *Nature Communications*, 9, 4569.

Zhao, Y., Li, L., Zheng, G., Jiang, W., Deng, Z., Wang, Z. et al. (2018) CRISPR/dCas9-mediated multiplex gene repression in *Streptomyces*. *Biotechnology Journal*, 13, e1800121.

## SUPPORTING INFORMATION

Additional supporting information can be found online in the Supporting Information section at the end of this article.

**How to cite this article:** Yang, M., Hao, Y., Liu, G. & Wen, Y. (2024) Enhancement of acyl-CoA precursor supply for increased avermectin B1a production by engineering meilingmycin polyketide synthase and key primary metabolic pathway genes. *Microbial Biotechnology*, 17, e14470. Available from: <https://doi.org/10.1111/1751-7915.14470>